

A short review of the magnetoelectric effect and related experimental techniques on single phase (multi-) ferroics

J.-P. Rivera^a

Department of Inorganic, Analytical and Applied Chemistry, University of Geneva, Sciences II, 1211 Geneva 4, Switzerland

Received 24 February 2009 / Received in final form 21 June 2009

Published online 10 October 2009 – © EDP Sciences, Società Italiana di Fisica, Springer-Verlag 2009

Abstract. Whereas materials with intrinsic magnetoelectric (ME) effects have not yet made inroads in technology, the measurement of their tensor characteristics has become a precious tool for magnetic point group determination. Therefore, it is worthwhile to consider different measurement techniques. In particular techniques for determining the linear and bilinear ME effects will be discussed, essentially the quasi-static and dynamic magnetic field-induced methods will be evaluated. The measurement and application of ME “butterfly” loops for determining (weak) ferromagnetism and internal bias fields will be described. For the bilinear ME effect (with invariant EHH) a particularly sensitive measurement method with amplification effect will be highlighted, permitting, e.g., to detect subtle magnetic phase transitions. At least for the linear ME effect, we will stress that in the future only a dimensionless quantity should be used which is valid in all systems of units. Finally, the linear ME effect of TbPO₄ crystals is reexamined because in a former publication it was not clear which system of units was effectively used (“rationalized” or “not rationalized” Gaussian system of units). Effectively, this crystal has the largest linear ME effect known. At $T = 1.50$ K, in SI units: α_{xy} or $\alpha_{yx} = 730$ ps/m, i.e., 0.220 in “not rationalized” Gaussian system of units.

PACS. 75.80.+q Magnetomechanical and magnetoelectric effects, magnetostriction – 61.50.Ah Theory of crystal structure, crystal symmetry; calculations and modeling – 75.30.K Magnetic phase boundaries – 75.50.Ee Antiferromagnetics – 06.20.F- Units and standards

1 Introduction

Multi-ferroic is a term coined by Schmid for crystals “in which two or all three of the properties ferroelectricity, ferromagnetism and ferroelasticity occur simultaneously in the same phase” [84,85,87]. In some crystals, the magnetoelectric effect (ME) is characterized by the appearance of an electric polarization \mathbf{P} under the application of a magnetic field \mathbf{B} (ME_B), for historical reasons also denoted by ME_H , with an applied field \mathbf{H} , or by the appearance of a magnetization \mathbf{M} under the application of an electric field \mathbf{E} (ME_E). If we consider only the linear ME effect, these vectors (\mathbf{P} and \mathbf{B} or \mathbf{M} and \mathbf{E}) are related by a second rank tensor α . The applied fields can be either quasi-static, dynamic or pulsed or even a combination of the first two. The appearance of such a ME effect, either linear or of higher order, is restricted by the magnetic point group (Heesch-Shubnikov group) of the crystal.

In this short review, we discuss first the phenomenology of the ME effect and the various systems of units we encounter and how to pass from one system to another one. Then we comment on the toroidal moment and the density of free energy. The complete tensor forms of the

linear ME effect will be given, in particular for the three monoclinic settings and the three orthorhombic ones. Direct measurement of the ME effect will be described, in particular the ME_B one, including a sensitive method to detect one of the bilinear ME effects. Finally, the linear ME effect of a TbPO₄ crystal was reexamined as it was not clear which system of units was used in former publications (Gaussian or “rationalized” Gaussian units). This material is known to possess the largest linear ME effect of all single crystals measured so far.

2 Phenomenology and system of units

2.1 The ME effect for bulk materials

2.1.1 Introductory remarks

Here, we will restrict ourselves to single crystals and, as far as possible, to single-domain-state – dielectric-crystals being in one or more of the following states: ferroelectric, paramagnetic or ferromagnetic, antiferromagnetic, ferrimagnetic or weakly ferromagnetic, ferroelastic. Until now, the ME effect of single crystals has not yet made

^a e-mail: Jean-Pierre.Rivera@unige.ch

inroads in technology. However, it is a very valuable complementary tool to neutron diffraction and crystal optics to study magnetic phase transitions. The ME effect may be a help to obtain accurate Néel temperatures (T_N) and to determine the magnetic point group via the form of the ME tensor(s) of the linear and/or the bilinear ME effect(s). Critical exponents may also tentatively be deduced [74]. The ME_B effect can be studied using even tiny crystals with an area of at least 0.5 mm^2 and, say, $50 \text{ }\mu\text{m}$ thickness or less, the thickness being not too critical. The ME_E effect can even be measured with smaller crystal size, using a SQUID system [15,51].

As an example, in a LiCoPO_4 single crystal [74], below and close to T_N , a so-called “butterfly loop” [87] indicated a probable lower symmetry than the one determined earlier [76] (mmm' , a “pure” antiferromagnet)¹. Thus, the existence of a spontaneous magnetization was first inferred via the measurement of the ME effect. These butterfly loops were confirmed using higher magnetic fields [52,101]. Measurements with a SQUID system [49,50] revealed a very weak magnetization. A new magnetic structure determination with neutron diffraction [99] showed a small tilting (4.6°) of the opposite spins out of the b axis, suggesting monoclinic symmetry. This crystal is in fact a weak ferrimagnet.

2.1.2 Linear ME effect

Although the ME effect has been conjectured in 1894 by Pierre Curie [21] and later by Landau and Lifshitz [53], it was Dzyaloshinskii who, in a short seminal paper [22], showed that this effect should exist in Cr_2O_3 crystals. He took into account neutron diffraction data of Cr_2O_3 crystals and determined the magnetic point group $3'm'$, which permits an antiferromagnetic phase below $T_N = 308 \text{ K}$. Dzyaloshinskii explicitly gave a phenomenological expression for the (density of a) thermodynamic potential expanded in terms of $E_i E_k$, $H_i H_k$ and the products $E_i H_k$.

Taking the partial derivative of this thermodynamic potential with respect to E_i and retaining only the ME effect terms, he obtained:

$$D_x = D_y = D_\perp = \alpha_\perp H_\perp$$

and

$$D_z = D_\parallel = \alpha_\parallel H_\parallel, \quad (1)$$

the z axis being parallel to the trigonal axis.

This paper by Dzyaloshinskii, published half a century ago, triggered theoretical and experimental investigations in ME effects, following some unsuccessful attempts made before, see O'Dell [61] for a historical introduction.

Soon thereafter, Astrov [7] found this effect in Cr_2O_3 , using a ME_E dynamic method. He measured $\alpha_{xx} = \alpha_{yy} \equiv \alpha_\perp(T)$ and $\alpha_{zz} \equiv \alpha_\parallel(T)$ as well as their relative signs [8]. The dynamic linear ME_E effect and the quasi-static converse effect (ME_H) were soon measured by Folen and collaborators [28,65,66] in Cr_2O_3 crystals.

¹ The prime (') denoting a time reversal operation added to the crystallographic symmetry element.

For the linear ME effect, α is a second rank tensor which changes sign under space inversion or time reversal and, accordingly, is invariant under simultaneous space and time inversion. In the most general case, for a triclinic crystal, this tensor has 9 independent components. It is asymmetric but can always be decomposed into a sum of a tracefree symmetric tensor, an antisymmetric tensor, and a pseudoscalar trace or, equivalently, into a pseudoscalar, a vector and a symmetric traceless tensor, see, e.g., [39,93]. The antisymmetric tensor part has only off-diagonal components. For that decomposition, we need to know at least the relative signs of all the components of the tensor α . The absolute signs relative to the signs of spontaneous polarization, magnetization and/or absolute crystallographic (with X-ray) or magnetic (with neutrons) space structures are more difficult to determine.

2.1.3 Linear and higher order ME effects

Hou and Blombergen [10,42] found in a piezoelectric paramagnetic crystal ($\text{NiSO}_4 \cdot 6\text{H}_2\text{O}$) a “paramagnetoelectric” effect (EHH) and O'Dell [60] measured a so-called “induced magnetoelectric effect” (HEE) in Y.I.G. (yttrium iron garnet) which were recognized by Ascher [3] as higher order ME effects.

We have, in the density of the free energy, to add these two higher order terms provided they are allowed by symmetry. Contrary to a common thought, these are generally by no means negligible at sufficient high magnetic fields at, say, 1 T:

(1/2) $\beta_{ijk} E_i H_j H_k$ and/or (1/2) $\gamma_{ijk} H_i E_j E_k$, linear in \mathbf{E} and bilinear in \mathbf{H} and/or linear in \mathbf{H} and bilinear in \mathbf{E} , respectively. We continue to use here the field \mathbf{H} , instead of the more appropriate field \mathbf{B} , for comparison purposes with published papers [39,40,61]. We use for convenience the symbol (β_{ijk}) of Rado [68] rather than the original one (α_{ijk}) of Ascher [3]. We do not want to have the same α symbol for the linear and one of these bilinear ME effects. Once a convention has been chosen for these three tensors, one has to be careful to respect the order of the indices relatively to the ones of \mathbf{E} and \mathbf{H} . These third rank tensors (β_{ijk} and γ_{ijk}) are necessarily symmetric in their last two indices, for example, $\beta_{i12} E_i H_1 H_2$ cannot be distinguished from $\beta_{i21} E_i H_2 H_1$. Actually, this can be deduced from thermodynamic relations. Thus, in the more general case for a triclinic crystal, from a total of 27 components either for the tensors β or γ , we are left with only 18 independent components. Very often, the last two indices $jk = 11, 22, 33, 23, 31, 12$ are replaced by one single index running from 1 to 6. For $\beta_{i\nu}$, for example, we have $i = 1, \dots, 3, \nu = 1, \dots, 6$, see, e.g., [31,33,59]. One has also to be careful to indicate whether or not a factor one half or two is included in the equations.

Phenomenologically, we can develop the density of the free energy into a series in \mathbf{E} , \mathbf{H} , and possibly the stress σ , for the field \mathbf{B} , see below. Using SI units (denoted below

with a left upper index: SI), see, e.g., [75], we have:

$$\begin{aligned}
-{}^{SI}g(\mathbf{E}, \mathbf{H}; T) = & \dots + P_i^s E_i + M_i^s H_i \\
& + (1/2)\varepsilon_0 \varepsilon_{ik} E_i E_k \\
& + (1/2)\mu_0 \mu_{ik} H_i H_k + {}^{SIH} \alpha_{ik} E_i H_k \\
& + (1/2){}^{SIH} \beta_{ijk} E_i H_j H_k \\
& + (1/2){}^{SIH} \gamma_{ijk} H_i E_j E_k \\
& + (1/6){}^{SIH} \delta_{ijk} E_i E_j E_k \\
& + (1/6){}^{SIH} \eta_{ijk} H_i H_j H_k + \dots \quad (2)
\end{aligned}$$

where \mathbf{E} is measured in V/m and \mathbf{H} in A/m, T stands for the temperature in K , ε_{ik} and μ_{ik} are dimensionless symmetric second rank tensors. Practically, for single domain ME crystals, the order of magnitude of ${}^{SIH} \alpha_{ik}$ is ps/m and the one of ${}^{SIH} \beta_{ijk}$ is as/A, \mathbf{P}^s is the spontaneous polarization, \mathbf{M}^s the spontaneous magnetization, ε_0 and μ_0 ($\equiv 4\pi \times 10^{-7}$ Vs/(Am)) are the vacuum dielectric permeability and vacuum magnetic susceptibility, respectively, with $\varepsilon_0 \mu_0 = 1/c^2$, where $c \approx 3 \times 10^8$ m/s is the speed of light in vacuum. This series expansion is valid because the external applied fields are small relative to the internal ones. Here, we added the last two terms, with third rank tensors, δ_{ijk} and η_{ijk} , because if we start with the 4-dimensional constitutive law of electromagnetism, these terms must appear in addition to the ones with β_{ijk} and γ_{ijk} [41], see also [47]. The factors 1/6 are inserted for convenience. These third rank tensors are totally symmetric in all their indices, i.e., $\delta_{ijk} = \delta_{ikj} = \delta_{jki} = \delta_{jik} = \delta_{kij} = \delta_{kji}$, the same for η_{ijk} . Thus from a total of 27 components for each tensor, we are left with only 10 independent components for a crystal of triclinic symmetry.

For Gaussian units (with left upper script index: G), which are not rationalized, a factor 4π appears in the denominator of the series development of $-g$. The Gaussian system of units is a mixture of the electrostatic cgs units (cgs esu) and the electromagnetic cgs units (cgs emu), see, e.g., [62,91], one has:

$$\begin{aligned}
-{}^Gg(\mathbf{E}, \mathbf{H}; T) = & \dots + (1/(4\pi)){}^G \alpha_{ik} E_i H_k \\
& + (1/(8\pi)){}^G \beta_{ijk} E_i H_j H_k \\
& + (1/(8\pi)){}^G \gamma_{ijk} H_i E_j E_k \\
& + (1/(24\pi)){}^G \delta_{ijk} E_i E_j E_k \\
& + (1/(24\pi)){}^G \eta_{ijk} H_i H_j H_k + \dots \quad (3)
\end{aligned}$$

here, with Gaussian units, \mathbf{E} must be measured in statvolt per centimeter and \mathbf{H} in oersted.

Sometimes, numerical tables are given in ‘‘rationalized’’ Gaussian units (with left upper script index: rG), which are, actually, pseudo-rationalized Gaussian, or ‘‘partial’’ Heaviside-Lorentz system of units, without the 4π factors in the above denominators.

The conversion of units from one system to another is easily done by computing the density of the free energy [75], a mechanical unit, as

$$g = 1 \text{ J/m}^3 = 1 \text{ kg/(s}^2 \text{ m)} = 10 \text{ g/(s}^2 \text{ cm)} = 10 \text{ erg/cm}^3,$$

we obtain the following relations [14,75]:

$$c {}^{SIH} \alpha = {}^G \alpha = 4\pi {}^{rG} \alpha \quad (4)$$

with c the speed of light in vacuum, ${}^{SIH} \alpha$ in s/m, but ${}^G \alpha$ and ${}^{rG} \alpha$ being dimensionless. For clarity, here, the lower right indices has been removed in equation (4). For the conversion of units in electromagnetism see, e.g., [17,27,38,44,54,62,91,98].

The polarization P_k is obtained by taking the partial derivative of $-g$ with respect to E_k , as mentioned above, and the magnetization M_k by taking the partial derivative of $-g$ with respect to H_k , see, e.g., [75],

$$\begin{aligned}
P_k(\mathbf{E}, \mathbf{H}; T) = & - \frac{\partial g}{\partial E_k} = \dots + P_k^s + \varepsilon_0 \varepsilon_{ki} E_i + {}^H \alpha_{ki} H_i \\
& + (1/2){}^H \beta_{kij} H_i H_j + {}^H \gamma_{ijk} H_i E_j + \dots, \quad (5)
\end{aligned}$$

$$\begin{aligned}
M_k(\mathbf{E}, \mathbf{H}; T) = & - \frac{\partial g}{\partial H_k} = \dots + M_k^s + \mu_0 \mu_{ik} H_i + {}^H \alpha_{ik} E_i \\
& + {}^H \beta_{ijk} E_i H_j + (1/2){}^H \gamma_{kij} E_i E_j + \dots \quad (6)
\end{aligned}$$

Other terms, to cite only a few, linear in \mathbf{E} and σ (stress) or \mathbf{H} and σ , with third rank tensors are responsible for the piezoelectric effect [59,94] discovered by the Curie brothers (1894) or the piezomagnetic effect. The first who postulated the piezomagnetic effect was Voigt [100]. He wrote down the tensor forms, however, since time reversal was not yet known at that time, those forms are inappropriate. Finally the piezomagnetic effect was first measured by Borovik-Romanov [13,14]². Note that the linear magnetostriction effect is the converse effect of the piezomagnetic one. Terms with a fourth rank tensor giving rise to electrostriction, linear in σ and bilinear in \mathbf{E} , or magnetostriction linear in σ and bilinear in \mathbf{H} , or even piezomagneto-electric effect, linear in \mathbf{E} , \mathbf{H} and σ , are not written down here. This last effect has been searched for by Rado [67] and by Rivera [73] without success. Grimmer [32] computed the forms of this fourth rank tensor for the allowed magnetic (Heesch-Shubnikov) point groups. A large ME effect was found in a spin-glass system [90], by using a ME SQUID susceptometer [15], additional ${}^H d_{ijkl} E_i E_j H_k H_l$ terms in the free energy density gave rise to a fourth rank tensor (${}^H d_{ijkl}$).

Other terms could be added to the series development of $-g$, due to the velocity \mathbf{v} of a moving dielectric under an electric field and/or a magnetic one, yielding $-g(\mathbf{E}, \mathbf{B}, \mathbf{v}; T)$ [6], see also [37]. Note that the matrix of the linear ME_E effect ($M_i = \alpha_{ki} E_k$) is the transpose of the matrix of the linear ME_H effect or more correctly ME_B , see below, ($P_i = \alpha_{ik} B_k$):

$${}^{MEE} \alpha = ({}^{MEB} \alpha)^t. \quad (7)$$

² Unfortunately, Nye still mentions in his textbook (1990 edition) [59], Table 23, Appendix C, p. 291, that the ‘‘existence of piezomagnetism [is] not firmly established’’!

Care must be exercised when giving or reading numerical coefficients in tables. The choice of units, SI, Gaussian (G) or even “rationalized” Gaussian (rG) is another source of errors due to a factor 4π (≈ 12.6) between these last two system of units. This is slightly more than an order of magnitude! Thus, the equation for the density of the free energy and the equation for the induced polarization or for the induced magnetization should always be explicitly given, otherwise one could have to repeat the experiments as the ME_H experiments on $TbPO_4$ cited below. This problem seems recurrent in magnetism as already mentioned in Landolt-Börnstein Tables by Zinn [103].

As to the choice of \mathbf{H} or \mathbf{B} , O’Dell gave convincing arguments in his book [61] why in the density of free energy ($-g$) one must use \mathbf{B} instead of \mathbf{H} , see also Post [63]. In the book by Sommerfeld [91] it is stressed that \mathbf{E} (electric field strength) and \mathbf{B} (magnetic field strength) are intensive variables or “intensities”, \mathbf{D} (electric excitation) and \mathbf{H} (magnetic excitation) are extensive variables or, as some authors call them now, “extensities”. For a discussion of intensive and extensive variables in thermodynamics see, e.g., [34,92,102]. It is not necessary to remind ourselves that \mathbf{E} and \mathbf{B} appear in the Lorentz force equation, see, e.g., [64]. In most modern textbooks in physics \mathbf{B} is the magnetic field. See also arguments given by Panofsky and Philips [62] pp. 143–144, based on experiments, why, in material sciences, \mathbf{B} is “more fundamental” than \mathbf{H} . Ascher [6], in a paper concerning kineto-electric and kineto-magnetic effects in crystals used \mathbf{B} and no more \mathbf{H} as in his previous papers. So, we must write:

$$-g(\mathbf{E}, \mathbf{B}; T) = \dots + P_i^s E_i + \varepsilon_0 \varepsilon_{ik} E_i E_k + {}^B M_i^s B_i + {}^B \alpha_{ij} E_i B_j + (1/2) {}^B \beta_{ijk} E_i B_j B_k + (1/2) {}^B \gamma_{ijk} B_i E_j E_k + \dots, \quad (8)$$

$$P_k(\mathbf{E}, \mathbf{B}; T) = -\frac{\partial g}{\partial E_k} = \dots + P_k^s + \varepsilon_0 \varepsilon_{ik} E_i + {}^B \alpha_{ki} B_i + (1/2) {}^B \beta_{kij} B_i B_j + {}^B \gamma_{ijk} B_i E_j + \dots, \quad (9)$$

also for

$$\mathbf{M} = \mathbf{M}(\mathbf{E}, \mathbf{B}; T). \quad (10)$$

In order to avoid the conversion of units, we can use a four-dimensional susceptibility tensor ξ . This tensor emerges in the linear relation between the four-dimensional polarization $\mathbf{M}_{\sigma\tau}$ and the field strength $\mathbf{F}_{\mu\nu}$ (O’Dell [61], Eqs. (2.45) and (2.51))

$$\mu_0 c \mathbf{M}_{\sigma\tau} = (1/2) \xi_{\sigma\tau}^{\mu\nu} \mathbf{F}_{\mu\nu}, \quad (11)$$

with $\mu, \nu, \sigma,$ and $\tau = 1, \dots, 4$ (space and time coordinate indices), from which one gets: $\mathbf{P} = (i/c) \xi \mathbf{H}$, with $i^2 = -1$. In these equations, ξ is dimensionless. O’Dell’s use of an imaginary time coordinate is outdated and should not be used. Already at MEIPIC1, Ascher [6] wrote down a dimensionless magnetoelectric tensor (λ_{ij})

$$-g(\mathbf{E}, \mathbf{B}; T) = \dots + \varepsilon_0 \lambda_{ik} E_i c B_k + \dots, \quad (12)$$

with a $-g$ function of \mathbf{E} and \mathbf{B} . After computing the partial derivative of $-g$ with respect to E_i , he already obtained

$$P_i = \dots + (\lambda_{ik})(1/R_0) B_k, \quad (13)$$

with R_0 as vacuum impedance. Accordingly, this equation is valid in any system of units.

Starting also with the four-dimensional electromagnetic field tensor Hehl and Obukhov obtained quantity equations valid in an arbitrary system of units. For the case of a Cr_2O_3 single crystal, below T_N , in relation to the so called Post constraint problem [63], equation (31) of [39] reads

$$D_z = \left(\varepsilon_{zz} - \frac{\alpha_{zz}^2}{\mu_{zz}} \right) \varepsilon_0 E_z + \frac{\alpha_{zz}}{\mu_{zz}} \sqrt{\frac{\varepsilon_0}{\mu_0}} B_z \quad (14)$$

and similar equations hold for the x and y axes but in these cases, $\varepsilon_x = \varepsilon_y = \varepsilon_\perp$ and $\alpha_x = \alpha_y = \alpha_\perp$. In all D_k equations ($k = \perp, z$), $\mu_k = 1 + \chi_k \approx 1.00$, as, e.g., $\chi_\perp(T_N) \approx 1.63 \times 10^{-3} \ll 1$ [39,61]. These α_{zz} and α_\perp are dimensionless (as are $\varepsilon_{zz}, \mu_{zz}, \dots$) and normalized by the vacuum impedance $R_0 = \sqrt{(\mu_0/\varepsilon_0)}$, see also [40]. In SI units, ${}^{SI}R_0, \approx 377 \text{ V/A (=ohm)}$.

If we had from the very beginning of the ME experiments introduced these dimensionless ME linear coefficients, we would have escaped all these problems of conversion of units, as for ε relative and μ relative (dimensionless) which are valid in any system of units. It is a pity that Ascher could not draw the attention to experimentalists to this problem already in the 1960s. These α (dimensionless), valid in any system of units, have, by chance, the same numerical value as ${}^G\alpha$ (dimensionless) in the Gaussian (not rationalized) system of units but not the same numerical values as ${}^{rG}\alpha$ in the “rationalized” Gaussian system of units, where they are also dimensionless!

If we write

$$-g(\mathbf{E}, \mathbf{B}; T) = \dots + {}^a \alpha_{ij} E_i B_j + \dots, \quad (15)$$

the ${}^a\alpha_{ij}$ components, not normalized by the vacuum admittance, have the dimension of an admittance [6,39,40] (hence the notation a), in SI units: $A/V = \text{siemens} = 1/\text{ohm}$.

Now, to resume the situation, it is easy to show that we have

$$\alpha = R_0 {}^a\alpha = {}^{SI}R_0 {}^{SIB}\alpha = c {}^{SIH}\alpha = {}^G\alpha = 4\pi {}^{rG}\alpha \quad (\text{dimensionless}), \quad (16)$$

where the lower right indices are removed for clarity. Nevertheless, giving the components of the linear ME effect in SI units, ${}^a\alpha$ (siemens) = ${}^{SIB}\alpha$ (siemens), with field \mathbf{B} , but no more ${}^{SIH}\alpha$ (s/m), with field \mathbf{H} [75], allows one to check more easily the experimental values of the components of the tensor of the linear ME effect.

Another drawback of single crystals is that usually the ME effect takes place only at low temperature. Thus, we need liquid nitrogen or even liquid helium to cool down

the crystal, which is not particularly favorable for applications. The Cr_2O_3 crystal is one of the few exceptions, being magnetoelectric up to $T_N = 308 \text{ K} = 35 \text{ }^\circ\text{C}$. Another drawback is, unfortunately, that in bulk single crystals, the ME effect is very weak. Brown et al. [16], see also [4], showed that the elements of the linear magnetoelectric tensor are thermodynamically limited by

$$\alpha_{ik} < 4\pi\sqrt{(\epsilon\chi_{ii} \text{ }^m\chi_{kk})}. \quad (17)$$

This relation has been generalized for other material coefficients [5].

2.2 The ME effect for composite materials

With the aim of engineering applications with much larger effect at room temperature, composite materials are synthesized, e.g., stacking of magnetic and ferroelectric thin layers (nanoscale heterostructures), mimicking a large ME effect via piezoelectricity and/or electrostriction and piezomagnetism and/or magnetostriction³. First results in this field, as far as we know, were reported in [95]. The pseudo-ME effect in these materials is in part responsible for the revival of interest in the ME effect and the huge increase of related publications. But these two-phase multiferroics without doubt will play an important role in future magnetoelectric devices. A small one-turn coil, for example, with a diameter as small as $50 \text{ }\mu\text{m}$ (presently maybe even less) can be manufactured on an electronic printed circuit. It creates pulsed (30 ns) magnetic fields of up to 40 T [97]! Magnetostriction is quadratic in H , but to quote [35]: "... , the magnetostriction at a particular bias field H_0 , can give rise to pseudo-piezomagnetism over a small range where the slope of the magnetostriction curve dS/dH can be assumed to be constant. ... Thus pseudo-piezomagnetism at a bias field H_0 can be expressed as: $S = qH, \dots$ ".

In composite materials, an incoherent system of units is frequently used in the measurement of the pseudo-linear ME effect α , mixing \mathbf{E} in mV/cm and \mathbf{H} in Oe to obtain a pseudo-linear ME voltage coefficient ${}^E\alpha$, under "open circuit" condition measurements, i.e., with $D = 0$. It follows from $D = \epsilon_0\epsilon E + \alpha H = 0$ that $E/H = -(\alpha/(\epsilon\epsilon_0)) \equiv {}^E\alpha$, we will denote it by ${}^{HE}\alpha$ in order to remind ourselves that we use the field \mathbf{H} . They obtain

$${}^{HE}\alpha_{ij} = E_i/H_j \quad \text{in mV}/(\text{cmOe}) \quad (18)$$

see, e.g., [12]! This is of course neither a SI nor a Gaussian system of units, we could call it a "technical" or a "bastard" system of units. Other authors use more consistently SI units $(\text{V/m})/(\text{A/m}) = \text{ohm}$, e.g., [35]. Thus, in "composite circles", their ME pseudo-linear coefficients ${}^{HE}\alpha$ have the dimension of an impedance (ohm), the inverse of the one in ME_H linear effect in single crystal, ${}^a\alpha$, which

have the dimensions of an admittance (siemens = $1/\text{ohm}$), measured at $E = 0$, instead of $D = 0$.

For the conversion to ${}^{SIH}\alpha$ (s/m), we have the equation [36]:

$${}^{SIH}\alpha = \epsilon\epsilon_0 {}^{HE}\alpha. \quad (19)$$

The best would be to use \mathbf{B} instead of \mathbf{H} , giving ${}^{SIBE}\alpha$ in $(\text{V/m})/(\text{Vs/m}^2) = \text{m/s}$, the dimensions of a velocity!

To take into account composite materials, we finally have, at least for the linear ME effect, and with $\mu \approx 1.00$:

$$\begin{aligned} A\alpha &= {}^A R_0 {}^A\alpha = {}^{SI}R_0 {}^{SIB}\alpha = c {}^{SIH}\alpha = G\alpha \\ &= 4\pi {}^r G\alpha = \epsilon {}^{EH}\alpha/R_0 \quad (\text{dimensionless}). \end{aligned} \quad (20)$$

For the bilinear ME term, $D_k = \dots + {}^B\beta_{kij} B_i B_j + \dots$, the SI units of the components of ${}^B\beta$ are $\text{A m}^2/(\text{V}^2 \text{ s}) = \text{m}^2/(\Omega^2 \text{ A s})$ or alternatively $\text{C}/(\text{m}^2 \text{ T}^2) = \text{Cm}^2/\text{Wb}^2$. In former publications, with $D_k = \dots + {}^B\beta_{kij} H_i H_j + \dots$, the SI units of ${}^H\beta$ are, as already mentioned, s/A .

In order to remove any uncertainty in tables and/or in publications, maybe it would be best to give also α and β in SI units, i.e., in $\text{C}/(\text{m}^2 \text{ T})$ and $\text{C}/(\text{m}^2 \text{ T}^2)$, respectively, with the magnetic field \mathbf{B} in T and D in C/m^2 .

For a review of ME effects emphasizing composite materials see, e.g., [26].

3 Some remarks on the toroidal moment and the density of free energy

Only rather recently, the notion of toroidal moment density \mathbf{T} has been recognized [23,30,93]. At least two non-collinear magnetic moments, or spins in the elementary cell with opposite direction, can give rise to a toroidal moment perpendicular to their plane. A current \mathbf{i} flowing in a solenoid bent into a torus also gives rise to a toroidal moment parallel to the torus axis, perpendicular to the plane of the torus. A ferrotoroidic order parameter gives rise to antisymmetric contributions to the magnetoelectric effect, but not necessarily the contrary. Sannikov showed that in the magnetic phases of orthorhombic boracites the antisymmetric part of the linear magnetoelectric tensor is proportional to the toroidal moment [77–80]. He explained the narrow peak observed in the temperature dependence of $\alpha_{32}(T)$ below and close to the magnetic phase transition of Co-Br [18], Co-I [20] and Ni-Cl [72] orthorhombic ($\text{m}'\text{m}2'$) boracites. Only one value of this peak was measured in the first experiment of the ME_H effect on Ni-I boracite [2] at a temperature just below T_N and with an opposite value to the other ones at lower temperatures. Later on more detailed ME_H experiments on Ni-I boracites showed more clearly the negative peak [19]. We call this $\alpha_{32}(T)$ of Ni-I boracites a pseudo-orthorhombic coefficient because it was recognized [70] that Ni-I boracite was actually of lower symmetry than orthorhombic ($\text{m}'\text{m}2'$), namely monoclinic (m'). This was based on observations on a $(001)_{\text{cubic}}$ cut of spontaneous Faraday rotation below T_N , showing some magnetic domains, see Figure 1 (colour picture only on the online document). It was possible to move these magnetic

³ In a personal communication, Harshé [36] wrote me: "... , all of the known magnetostrictive materials do not exhibit any linear piezomagnetic effect".

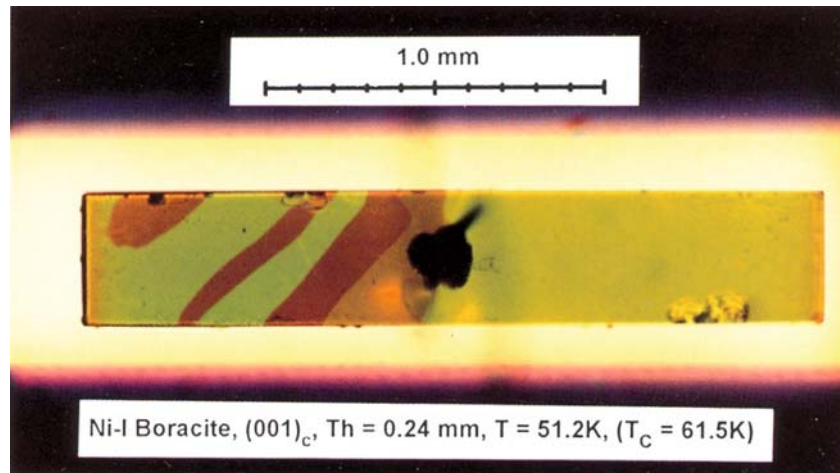


Fig. 1. (Color online) A pseudo (001) orthorhombic cut of Ni-I boracite, at $T = 51.2$ K below $T_N = T_C = 61.5$ K, obtained from a (001) cubic cut at room temperature [70]. Thanks to the spontaneous Faraday effect it shows magnetic domains, these magnetic bubbles were moveable with a small magnet outside of the cryostat. Polarized light, with the crystal oriented close to extinction, the analyzer being slightly uncrossed relatively to the polarizer. The central spot is the contacted gold (~ 70 μm dia.) wires to the semi-transparent gold deposited electrodes. Silver paste electrodes would not have allowed us to observe these domains.

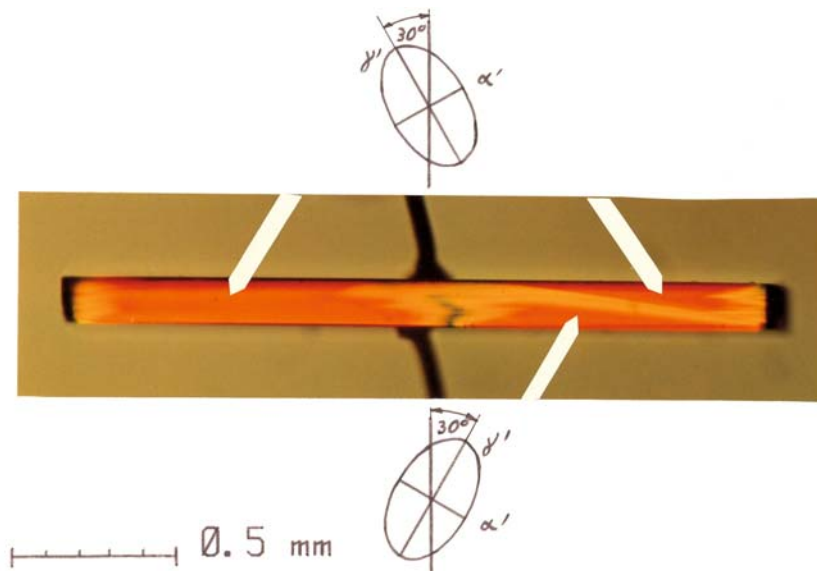


Fig. 2. (Color online) Another Ni-I boracite crystal, below T_N , showing stacking of domains, typical of a monoclinic phase and the possibility of switching the optical indicatrix direction with an applied \mathbf{E} field. The stacking of very fine lamellar domains are best seen directly through the polarized light microscope (PLM). This is a (110) cubic cut at 300 K and a pseudo (100) or pseudo (010) orthorhombic cut below T_N .

domains, close to T_N , using a small magnet (e.g., NdFeB magnet) outside of the cryostat. An orthorhombic phase ($m'm2'$) would not show on this cut such magnetic domains. Moreover, perpendicularly to a pseudo (110)_{cubic} cut, a rotation of the optical indicatrix of about $\pm 30^\circ$ was found (Fig. 2) by switching the component of the spontaneous polarization along a $[001]_{\text{pseudocubic}}$ direction, on applying a $\pm \mathbf{E}$ field along this direction. This is definitively not consistent with an orthorhombic symmetry. Note that Ni-I boracite is particularly interesting because it is the first ferroelectric, weak-ferromagnet (but essentially an antiferromagnet), magnetoelectric, which has

the same ferroelectric-Curie temperature and Néel temperature [2], $T_C \approx T_N \approx 61.5$ K [70]. The temperature was measured with a calibrated Carbon-Glass Resistor placed very near (about 8 mm) to the crystal in a cryostat with low pressure of He gas, as thermal exchange gas. In [2,81], it was shown that \mathbf{M}^s can be rotated, by about 90° , by reversing the main component of \mathbf{P}^s .

Continuing now with the toroidal moment \mathbf{T} , we should be very cautious not to add in $-g$ explicitly a term proportional to $\mathbf{T} \cdot \mathbf{S}$ (scalar product), with $\mathbf{S} \equiv \mathbf{E} \times \mathbf{H}$ (cross product of \mathbf{E} and \mathbf{H}) and not write $-g(\mathbf{E}, \mathbf{H}, \mathbf{S}, \sigma; T)$, as for example in [87], because \mathbf{S} is not a new

independent variable as could be, e.g., \mathbf{v} , \mathbf{j} or $\text{grad } M$ [6]. We cannot compute $-\partial g / \partial S_k$, for obtaining the spontaneous toroidal moment components T_k , because the S_k are functions of the \mathbf{E} and \mathbf{H} components, by definition.

If we add to $-g$, as in [87], terms of the form

$$\dots + \lambda_{ii} T_i S_i + \theta_{ij} S_i E_j + \zeta_{ij} S_i H_j + \dots \quad (21)$$

and substitute into them the components of S_k ,

$$S_1 = (E_2 H_3 - E_3 H_2), \quad S_2 = (E_3 H_1 - E_1 H_3)$$

and

$$S_3 = (E_1 H_2 - E_2 H_1), \quad (22)$$

one obtains:

$$\begin{aligned} -g = & \dots + \lambda_{11} T_1 (E_2 H_3 - E_3 H_2) \\ & + \lambda_{22} T_2 (E_3 H_1 - E_1 H_3) \\ & + \lambda_{33} T_3 (E_1 H_2 - E_2 H_1) \\ & + 18 \text{ terms in } \theta_{ij} f_{ij}(\mathbf{E}, \mathbf{H}) \\ & + 18 \text{ terms in } \zeta_{ij} k_{ij}(\mathbf{E}, \mathbf{H}) + \dots, \end{aligned} \quad (23)$$

where $f_{ij}(\mathbf{E}, \mathbf{H})$ and $k_{ij}(\mathbf{E}, \mathbf{H})$ are complicated functions of the components of \mathbf{E} and \mathbf{H} .

Let's compute the derivative of $-g$ with respect to E_k , to obtain P_k (with "Maple"™, a software for symbolic mathematical computation [58]). We only show the P_1 components:

$$P_1(\mathbf{T}, \mathbf{H}) = -\lambda_{22} T_2 H_3 + \lambda_{33} T_3 H_2, \quad (24)$$

$$\begin{aligned} P_1(\theta, \mathbf{H}, \mathbf{E}) = & 2(\theta_{13} H_2 - \theta_{12} H_3) E_1 + (-\theta_{13} H_1 \\ & + \theta_{23} H_2 + (\theta_{11} - \theta_{22}) H_3) E_2 \\ & + (\theta_{12} H_1 + (-\theta_{11} + \theta_{33}) H_2 - \theta_{32} H_3) E_3 \end{aligned} \quad (25)$$

and

$$\begin{aligned} P_1(\zeta, \mathbf{H}, \mathbf{E}) = & (-\zeta_{12} H_3 + \zeta_{13} H_2) H_1 \\ & + \zeta_{23} H_2^2 + (\zeta_{33} - \zeta_{22}) H_3 H_2 - \zeta_{32} H_3^2 \end{aligned} \quad (26)$$

we see that in the most general case, for a triclinic magnetic point group, we have only 2, 8 and 5 terms, respectively. The other components of \mathbf{P} , i.e., P_2 and P_3 , were also computed with Maple but could be simply obtained by cyclic permutation of the indices. Note that $P_k(\theta, \mathbf{E}, \mathbf{H}; T)$ is only a special case of $P_k(\mathbf{E}, \mathbf{H}; T) = \gamma_{kij} E_i H_j$, the ME effect linear in \mathbf{E} and \mathbf{H} and for which no E_k^2 components are effective. $P_k(\zeta, \mathbf{E}, \mathbf{H}; T)$ is also a special case of $P_k(\mathbf{E}, \mathbf{H}; T) = \xi_{kij} H_i H_j$, for which we have no component in H_k^2 . Similar results (not shown) are obtained concerning the magnetization due to the toroidal moment. Instead of computing the magnetization, we could have permuted the role of \mathbf{E} and \mathbf{H} , the role of θ and ζ and changed the signs of the terms in the above equations for the polarization.

Thus, the addition of such terms to the density of free energy is redundant until we have a detailed theory of the toroidal and ME effect. This redundancy was already pointed out, intuitively, in [87].

For recent reviews on toroidal moments in condensed-matter physics and its relation to the ME effect see [23,55,93].

Until now, it seems that no direct measurements of the toroidal moment were undertaken. Only indirect methods are known, as for example, the detection of the peak of the $\alpha_{32}(T)$ ME coefficients just below T_N in some boracite crystals, already mentioned and well explained by the theory of Sannikov, or the observation of toroidal and weak ferromagnetic (essentially antiferromagnetic) domains by optical second harmonic generation (SHG) by van Acken et al. [1]. In [87] it is explained that we do not have two different kinds of domain in LiCoPO_4 , i.e., "antiferromagnetic" and "ferrotoroidic", as assumed in [1], but that all four occurring domains are equivalent, i.e., they are all "ferrotoroidic and weakly ferromagnetic". The different contrast formation of the magnetic SHG signal was in fact caused by two different kinds of mutual spatial orientation of the "weakly ferromagnetic/ferrotoroidic" domains [87].

4 Magnetic symmetries

For a long time, in crystallography, only space inversion was considered in addition to other symmetry elements (axes, mirror planes, etc.) to establish the list of the 32 point groups (Hessel (1830), Bravais (1848)) and the 230 space groups (Fedorov (1890), Schönflies (1891)) [43]. Adding time reversal, one obtains 122 magnetic point groups (Heesch (1930), Shubnikov (1951)) and 1651 magnetic space groups (Zamoraev (1952), Belov, Neronova and Smirnova (1955)). See the recent paper by Litvin "Tables of crystallographic properties of magnetic space groups", reference [56], and his electronic book: "Magnetic Space Groups" [57].

Magnetic point groups admitting several physical properties as spontaneous polarization, anti-, ferromagnetism (and weak ferromagnetism), linear and/or bilinear ME effects, etc., are tabulated in many books or publications. But, as far as we know, one of the most useful ones for experimentalists (and theoreticians!) is Table II, by Schmid, "Classification of the 122 Shubnikov groups according to magnetoelectric types" [83]. A too much abbreviated version appeared in Tables 1.5.8.3. "Classification of the 122 magnetic point groups according to magnetoelectric types" [14], p. 140. One can find also an adaptation of Table II [83] in "Table 2. Classification of the 122 Heesch-Shubnikov point groups", in reference [87]. Nevertheless, and following Ederer [24], all the 122 magnetic point groups allow antiferromagnetism. See also Tables 4–8, Magnetic point groups in reference [96], p. 304.

There are 58 magnetic point groups allowing the linear α ME effect, 66 allowing the bilinear β ME effect and 66, with partial overlap with the preceding ones, allowing the bilinear γ ME effect, see Table II [83] or Table 2 [87]. Many former published tables with the tensor forms of the linear α ME effect have been corrected in [75]. Borovik-Romanov and Grimmer in [14] gave only a partial table of the tensor forms of the linear effect. The forms had

Tensor Forms of the Linear Magnetolectric Effect (L1).				
#1	$\bar{1}$			
2	1 1'			
(#2)	(2) (m') (2/m')	1 st setting		
0	$\parallel z \perp z \parallel \perp z$			
#3	2 m' 2/m'	2 nd setting		
3	$\parallel y \perp y \parallel \perp y$			
(#4)	(2) (m') (2/m')	3 rd setting		
0	$\parallel x \perp x \parallel \perp x$			
(#5)	(2') (m) (2'/m)	1 st setting		
0	$\parallel z \perp z \parallel \perp z$			
#6	2' m 2'/m	2 nd setting		
3	$\parallel y \perp y \parallel \perp y$			
(#7)	(2') (m) (2'/m)	3 rd setting		
0	$\parallel x \perp x \parallel \perp x$			
#8	222 (2m'm') (m'2m') m'm'2 m'm'm'			
3	$\parallel x \parallel y \parallel z \perp x \perp y \parallel z \parallel x \perp y \perp z \perp x \parallel y \perp z \perp x \perp y \perp z$			
#9	2'2'2 mm2 (2'mm') (m'2'm') mmm'			
3	$\parallel x \parallel y \parallel z \perp x \perp y \parallel z \parallel x \perp y \perp z \perp x \parallel y \perp z \perp x \perp y \perp z$			
#10	(2'2'2') (m2m) mm'2' (2'm'm) (mm'm)			
1	$\parallel x \parallel y \parallel z \perp x \perp y \perp z \perp x \perp y \parallel z \parallel x \perp y \perp z \perp x \perp y \perp z$			
(#11)	(2'2'2') (2mm) (m'2'm) (m'm'2') (m'mm)			
0	$\parallel x \parallel y \parallel z \parallel x \perp y \perp z \perp x \perp y \perp z \perp x \perp y \parallel z \perp x \perp y \perp z$			
15				

Tensor Forms of the Linear Magnetolectric Effect (L2).			
#12	4 $\bar{4}$ ' 4/m' 3 $\bar{3}$ ' 6 $\bar{6}$ ' 6/m'		
8			
#13	4' $\bar{4}$ ' 4'/m'		
3			
#14	422 4m'm' [$\bar{4}$ '2m' $\bar{4}$ 'm'2] 4/m'm'm'		
11	32 3m' $\bar{3}$ 'm'		
#15	622 6m'm' [$\bar{6}$ 'm'2 $\bar{6}$ '2'm'] 6/m'm'm'		
5	4'2'2 4'mm' $\bar{4}$ m2 $\bar{4}$ 2'm' 4'/m'mm'		
[#16]	$\parallel z \parallel x \perp d \parallel z \perp x \perp d \parallel z \parallel x \perp d \parallel z \parallel x \perp d \parallel z \perp x \perp d$		
0	[4'2'2 4'mm' $\bar{4}$ m2 $\bar{4}$ 2'm' 4'/m'mm']		
#17	42'2' 4mm [$\bar{4}$ '2'm' $\bar{4}$ 'm'2] 4/m'mm		
11	32' 3m' $\bar{3}$ 'm'		
#18	62'2' 6mm [$\bar{6}$ 'm'2' $\bar{6}$ '2'm'] 6/m'mm		
5	23 m'3' 432 $\bar{4}$ '3m' m'3'm'		
43 + 15 = 58			

KEY TO NOTATION
 • zero component
 • non-zero component
 • equal components
 • components with equal modulus but opposite sign

Fig. 3. Tabulation (L1 and L2) of the 18 possible tensor forms of the linear ME effect, including the three settings for the monoclinic symmetries, with the binary axis (2 or 2') either parallel (//) or perpendicular (\perp) to the z , y or x crystallographic axes, respectively. For the monoclinic symmetries, the recommended “standard” setting is the one with the binary axis parallel to the y axis or perpendicular to the monoclinic plane. Non “standard” crystallographic point groups are in parentheses. As to the orthorhombic symmetries, the recommended setting is the one with the binary axis parallel to the z axis. But when we have phase transitions as a function of temperature, it is essential to know all the possible tensor forms, as it was important when studying the case of LiCoPO_4 crystals [99].

been computed by Grimmer using the Fumi’s “Direct-Inspection Method” [29], see also [9]. They gave only one setting for the monoclinic magnetic point groups, which is not enough when we have a crystal having magnetic phase transitions as a function of temperature. In more recent papers, Schmid [86,87] reproduced the table of the tensor forms of α [75] with slight modifications in the presentation by asking me to take into account also the third setting of the monoclinic magnetic point groups. These tensor forms are reproduced above for convenience (Fig. 3), but with indication of the crystallographic axes (x , y or z) underneath some symmetry elements. They are either parallel (//) or perpendicular (\perp) to these symmetry elements.

The bilinear ME effect with the β_{ijk} , also denoted by $\beta_{i\mu}$, and γ_{ijk} (or $\gamma_{i\mu}$) third rank tensors have the same forms [3] as the piezoelectric [94] and piezomagnetic [14] tensors, respectively. Grimmer in [33] gave the transposed

forms of these tensors, by including also the toroidal effects.

Depending on the experimentally determined tensor forms of the linear and/or the bilinear ME effects, some possible magnetic point groups can be inferred, by using only tiny single domain crystals, and can usefully complement usual neutron and/or X-ray diffraction methods.

Recently, magnetic SHG was also shown to be a powerful complementary method for the determination of complex magnetic structures, such as that of hexagonal manganites [25]. This method is even a more local probe than the ME effect.

5 Direct measurement of the ME effect

For antiferromagnets $\mu_k \approx 1.00$, as we saw for Cr_2O_3 , but for weak ferromagnets, ferrimagnets or ferromagnets as, e.g., magnetite crystals, this simplification is certainly not fully justified. In these cases, we obtain only effective

components of the ME tensors. It is known by experience, that weak-ferromagnets, as boracite crystals, have to be clamped with some “Scotch tape” or glued on a small sample holder before applying a magnetic field in a ME experiment. Otherwise, even a small platelet may be subject to a torque with a magnetic field of a few tens of tesla or less. Another point should be mentioned, the demagnetizing field is usually never taken into account in ME experiments because of irregularly shaped platelets used, resulting here, too, in effective components of the ME tensors.

Deposition of semi-transparent gold electrodes applied to a crystal is mandatory before ME experiments. It is recommended not to apply silver paste electrodes because the effective area is smaller than imagined as demonstrated by transmission light microscopy. Silver paste electrodes are also less effective for polarizing a crystal and they induce strains at low temperature. At room temperature, LiF salt water electrodes seem to be most efficient for polarizing a crystal [82].

5.1 ME_B quasi-static experiments

O’Dell [61] mentions that the ME_B method is better than the ME_E one, because a higher energy density can be created with a magnetic field rather than with an electric field. It is also easier to apply a high magnetic field than a high electric field. With ME_E measurements there is always a risk of an electrical breakdown. With the quasi-static ME_B method at constant temperature, and if we measure the charges with an electrometer in charge mode, the electrometer input is at virtual ground ($E_{input} \approx 0$), so a small crystal conductivity is less critical than if we measure a voltage. Another possibility to overcome this problem of conductivity is to use pulsed magnetic fields.

In any case, before measuring the ME effect, it is mandatory to cool the crystal by so-called ME annealing, see, e.g., [89].

The quasi-static ME_B method consists in the application to a crystal of a slowly varying magnetic field with a rate of about 0.05 to 0.5 T/min. We first start by measuring $Q(t)_{B=0}$, with $B \cong 0$, for half a minute. Then, we increase B linearly vs. time, from 0 to about 1 T, stabilizing B at this value for half a minute. We decrease B linearly to 0 and finally we continue to measure the charges for about half a minute with $B = 0$. With this method, see an example in Section 6 (Fig. 6) below, we obtain, with $B \cong 0$ before and after the experiment, an oblique base line as in optical absorption spectroscopy experiments. The base line can be used to correct (subtract) the measured curve. The origin of this drift can be due to a component of the spontaneous polarization, when present, i.e., a pyroelectric signal when T is not absolutely stable. Whenever possible, temperature should be kept stable to about ± 0.03 K. In a pyroelectric crystal, not necessarily ferroelectric, the magnetic field induced polarization of the linear effect, say along a z -axis, for a field of 1 T, may be about thousand times smaller than the spontaneous polarization along this same axis. Thus crystals with a spontaneous polarization

parallel to the magnetically-induced polarization can disturb for a while ME_B measurements. Another origin of drift during quasi-static ME_B measurements can be due to small movements of the coaxial cables inside the cryostat (i.e., triboelectricity). It is necessary to use low noise coaxial cables, the impedance of which is not too critical at frequencies below, say, 10 kHz, usually they have 50 Ω . These low noise coaxial cables have a conductive graphite ribbon or foil between the central isolation and the external electrical shield.

Calibrated Carbon Glass Resistors are very convenient to measure the temperature as they have a monotonic temperature variation of the electrical resistance, for example a CGR2000TM from Lake Shore, has a resistance of about 10 ohm at room temperature increasing to 2000 ohm at 4.2 K. CGRs are not too much sensitive to magnetic fields, at least up to 1 T. A four point technique must be used to measure the electrical resistance of a CGR by applying a known current, about 1 mA at 300 K and only 10 μ A at 4 K, and measuring the voltage. In order to suppress any thermocouple effects at wire soldering and connectors, it is wise, for each temperature measurement, to reverse automatically the sign of the current, measure again the voltage and then compute the mean resistance. Calibrated GGRs could be obtained with tables of their Chebyshev coefficients allowing to compute automatically the CGR electrical resistance and then the temperature. Other new miniature temperature sensors are now available on the market, but for example, silicon resistors can only be used above 25 K. Below 4 K, it is advantageous to measure the temperature with a capacitive helium pressure meter. The pressure inside the crystal sample chamber is lowered by pumping over a small quantity of liquid He with rather large diameter tubes. Using a special valve, the He gas pressure inside this chamber can be stabilized. It is advantageous to protect the sample from gas turbulence by a small non-magnetic metal can around the crystal but having small holes for pressure compensation.

A very high input impedance electrometer must be used, in charge mode, with a sensitivity close to the femtocoulomb range. This depends of course on the area of the crystal and the order of magnitude of the ME coefficients. In charge mode, the electrometer works as having a virtual ground, thus $E_{input} \approx 0$, as already mentioned. Needless to say that cables, sample holder and connectors must be kept very clean for having an impedance as high as possible. The electrometers generally have a humidity absorbing compound in their head module. The DC or quasi-static charges $Q(B)$ are converted to an AC signal for easier amplification. Former electrometers were built with a low frequency (tens of hertz) mechanical vibrating plate condenser to convert the DC signal to an AC one. Now MOS-FET or other electronic components are used.

Magnetoelectric annealing by applying simultaneously \mathbf{B} and \mathbf{E} fields when cooling the crystal is mandatory, otherwise the ME signal is strongly diminished due to ferroelectric and/or ferro- and/or antiferromagnetic opposite domains. Experimentally, it is found that a magnetic field is more efficient than an electric field, as already

mentioned. Preliminary experiments with a polarizing microscope or with a SHG setup and an optical cryostat, allowing observation of domains down to 4 K, whenever possible, is also very important. An optical cryostat for simultaneous measurement of the quasi-static ME effect and optical domain checking appeared to introduce too much electrical noise, at least as concerns quasi-static ME experiments.

5.2 ME_B dynamic experiments

The ME_B dynamic method is realized by applying, with Helmholtz coils outside the cryostat, a low frequency ($f = 70$ to 140 Hz) magnetic field b_0 (5 to 20×10^{-4} T_{rms}) and if necessary simultaneously a DC magnetic bias field B_0 .

When \mathbf{B}_0 and \mathbf{b}_0 are parallel, the total magnetic field is, with $\omega = 2\pi f$,

$$B = B_0 + b_0 \sin(\omega t). \quad (27)$$

As the magnetic field-induced polarization is $P = \alpha B + \beta B^2$, one obtains

$$P = (\alpha B_0 + \beta B_0^2 + \beta b_0^2/2) + (\alpha b_0 + 2\beta b_0 B_0) \sin(\omega t) - (1/2)\beta b_0^2 \cos(2\omega t). \quad (28)$$

A “lock-in” amplifier “clamped” at the fundamental excitation frequency f , gives a “root mean square” voltage proportional to $(\alpha b_0 + 2\beta b_0 B_0)$. The phase of the “lock-in” amplifier must be carefully adjusted. If $\alpha \approx 0$, this method with a DC magnetic field B_0 boosts the dynamic detection of the bilinear or quadratic ME β_{ijk} components. The gain compared to the detection of the signal at $2f$, proportional to $\beta b_0^2/2$, with $B_0 \approx 1$ T and $b_0 \approx 0.002$ T, is $4B_0/b_0 \approx 2000$. This method was applied successfully to enhance, via the quadratic ME_B component β_{333} , the detection of two magnetic phase transitions in Cr-Cl boracite, at $T_{N1} = 9.7$ K and at $T_{N2} = 13.5$ K, respectively [75]. The β_{333} pseudo-coefficient presented, at the $T_{N1} = 9.7$ K magnetic phase transition, a marked peak, see Figure 4, possibly related to the existence of a toroidal moment. As far as we know, no theory can explain the effect of a toroidal moment on the bilinear ME effect. For details concerning the sequence of phase transitions in Cr-Cl boracite see references [75,88].

With the ME_B dynamic method, by sweeping B_0 , a false linear ME effect could be mimicked. This is why one has always to start with the quasi-static ME_B effect, with angular measurements $Q(\varphi)$, at constant magnetic field, then by sweeping slowly the B field to see if we have a linear and/or a bilinear ME effect and compute its or their value(s).

ME_E measurements will not be discussed as we have no experience with this method, but we only mention that by measuring the induced magnetization with a low frequency electric field e_{AC} applied to a platelet, and sometimes superimposed with a DC electric field E_{DC} as well as a DC magnetic field B_{DC} , can give complex signals, which is a source of errors. ME_E experiments are now usually performed with a SQUID device [15,51].

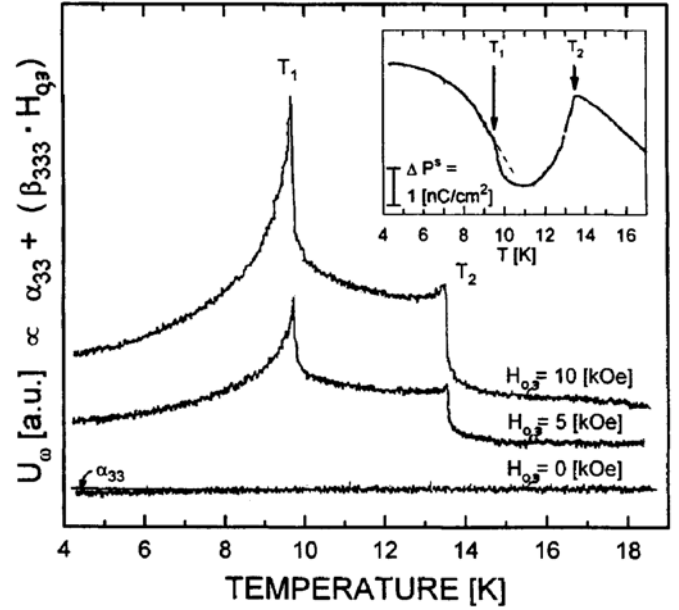


Fig. 4. Temperature dependence, at a rate of 2 K/min, of the pseudo β_{333} coefficient of the quadratic ME effect of Cr-Cl boracite measured dynamically with DC magnetic fields of 0, 5 and 10 kOe, superimposed to the AC magnetic field. The “boost” effect of H_0 on the detection of $\beta_{333}(T)$ is well exemplified, the noise being the same in each run. Two magnetic phase transitions are easily detected. The inset shows the detail of measurement of the spontaneous polarization.

Moreover, the ME_E method needs a calibration of the experimental set-up, which is not the case for the ME_B method. In order to find the magnetoelectric components of α and β with this latter method, we only measure the area of the crystal platelet, the magnetic field and the induced charges.

The detection of the so-called “butterfly” loop ($Q(B)$, $-B_{cor} < B < +B_{cor}$, where B_{cor} is the coercive field) was shown for the first time in Figure 4 of reference [2], see also [81], called at that time “quadratic magnetoelectric hysteresis loop” although it concerned the linear ME effect of a Ni-I boracite crystal and was not at all quadratic. Such a “butterfly” loop is the signature of (weak) ferromagnetism, the magnetic domains switching back when the magnetic field $|B|$ is greater than the magnetic coercive field $|B_{cor}|$, changing the sign of the slope of $Q(B)$. Such “butterfly” loops were found in other boracite crystals, e.g., in Ni-Br boracites [71], and in LiCoPO₄ [74] single crystal, at $T = 21.5$ K and at $T = 21.8$ K, thus below and very close to $T_N = 21.9$ K. This was confirmed at lower temperature and higher magnetic fields [52,101]. In previous works [76], it was found that LiCoPO₄ had a magnetic symmetry allowing “true” antiferromagnetism. New neutron scattering [99] and SQUID measurements of a weak magnetization [48,50] confirmed a lowering of symmetry from mmm' to $2'$.

When single crystals are not at hand or if unpolarizable polydomain crystals are available only, linear ME effect measurements are possible on insulating powders and can

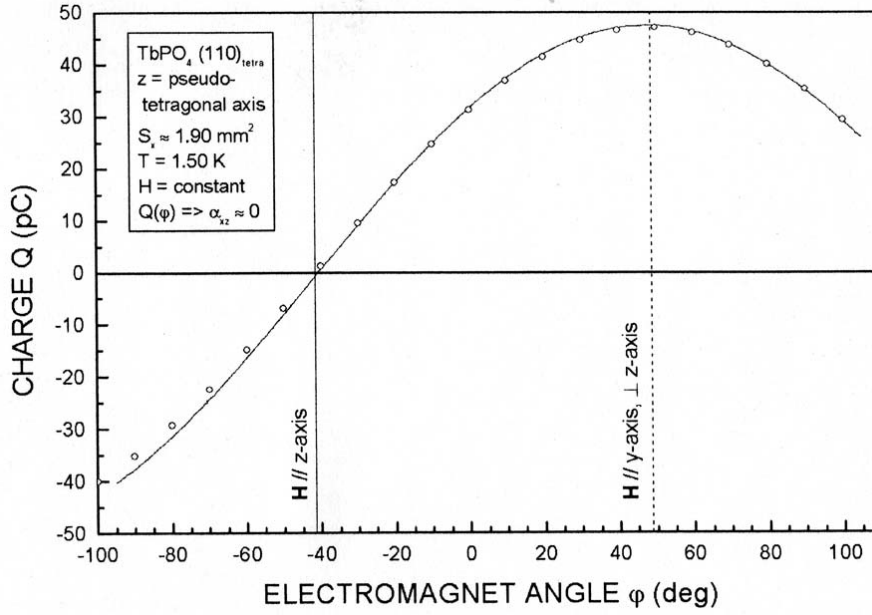


Fig. 5. $\text{TbPO}_4 (110)_{tetra}$ single crystal after ME annealing. Angular charges Q measurement, at $T = 1.50$ K, vs. the angle φ of the magnetic field in a plane of the monoclinic y -axis (or x -axis) and the z -axis. The z -axis is parallel to the tetragonal z -axis and the x and y axes are at 45° to the tetragonal a and a' axes. The open circles are computed and normalized points of a sine function of the orientation of the magnetic field.

yield information, whether diagonal, off-diagonal or both diagonal and off-diagonal ME coefficients are present [89].

6 Example of a ME_B measurement: TbPO_4

At room temperature TbPO_4 has a tetragonal zircon structure $I4_1/amd (4/mmm1')$. It is known that two magnetic phase transitions take place at low temperature in a narrow temperature range. Between T_{N1} and T_{N2} the magnetic symmetry is tetragonal $4'/m'mm'$, with T_{N1} being the upper magnetic phase transition to the paramagnetic phase. Below T_{N2} , the symmetry is most probably monoclinic $2'/m$ [11], with a unit cell (x, y) rotated by 45° around the tetragonal axis (z -axis). A detailed analysis of the domains in this phase is described in [11]. This type of crystal was repeatedly measured in the past [11,69] because it was claimed to have at low temperature the largest linear ME effect of any crystals. Unfortunately, it was not clear whether not rationalized Gaussian or rationalized Gaussian units were used in [69]. In [11,45] and [46] only relative values of $\alpha(T)$ were measured and discussed. Here, two crystals of TbPO_4 , a (110) tetragonal crystal cut (# 1: $S_x \approx (1.90 \pm 0.10) \text{ mm}^2$, thickness $t_y \approx (340 \pm 6) \mu\text{m}$) and a (100) tetragonal crystal cut (# 2: $S_a \approx ? \approx 60\% S_x$, $t_{a'} \approx (280 \pm 6) \text{ mm}$) were prepared and gold evaporated from samples kindly supplied, in 2001, by Kahle, University of Karlsruhe. The results described below were never published.

6.1 First step

In Figure 5, crystal #1, the first experiment after the ME annealing on cooling was to measure the ME signal vs. the angle of the magnetic field. The orientation of the electromagnet was simply recorded by fixing a wheel on the axis of a 15 turns potentiometer, a linear variable resistor with a maximum resistance of 50 k Ω , fixing this system on the base of the electromagnet turn table and by measuring the voltage proportional to the angular position. At $T \approx 1.50$ K, the magnetic field was rotated in the plane formed by the pseudo tetragonal z -axis and the monoclinic y -axis (it could be the x -axis). We observed a “true” sinusoidal curve by measuring the quasi-static signal $Q(\varphi)$, at constant amplitude of H , with an electrometer in charge mode. The maximum signal is obtained for α_{xy} (or α_{yx}) when \mathbf{H} is oriented perpendicularly to the pseudo-tetragonal z -axis. For \mathbf{H} parallel to the z -axis the signal was zero, thus α_{xz} (or α_{yz}) is zero.

6.2 Second step

It was necessary to verify whether the ME effect is only linear (Fig. 6). The procedure was already described in the preceding Section 5. It is evident from Figure 6 that we have only a linear component. From the difference of the charges at H_{max} and at H_{min} , corrected for a slight drift, we can compute the linear ME component α_{xy} (or α_{yx}), in SI units: $\alpha_{xy}(1.50 \text{ K}) = \Delta Q / (S_x \Delta H_y) \approx 730 \text{ ps/m}$ and by multiplying with $c \approx 3 \times 10^8 \text{ m/s}$ we obtain the Gaussian value: $\alpha_{xy}(1.50 \text{ K}) \approx 0.220$, or, in the “rationalized” Gaussian units, 0.0174. This last value is obtained

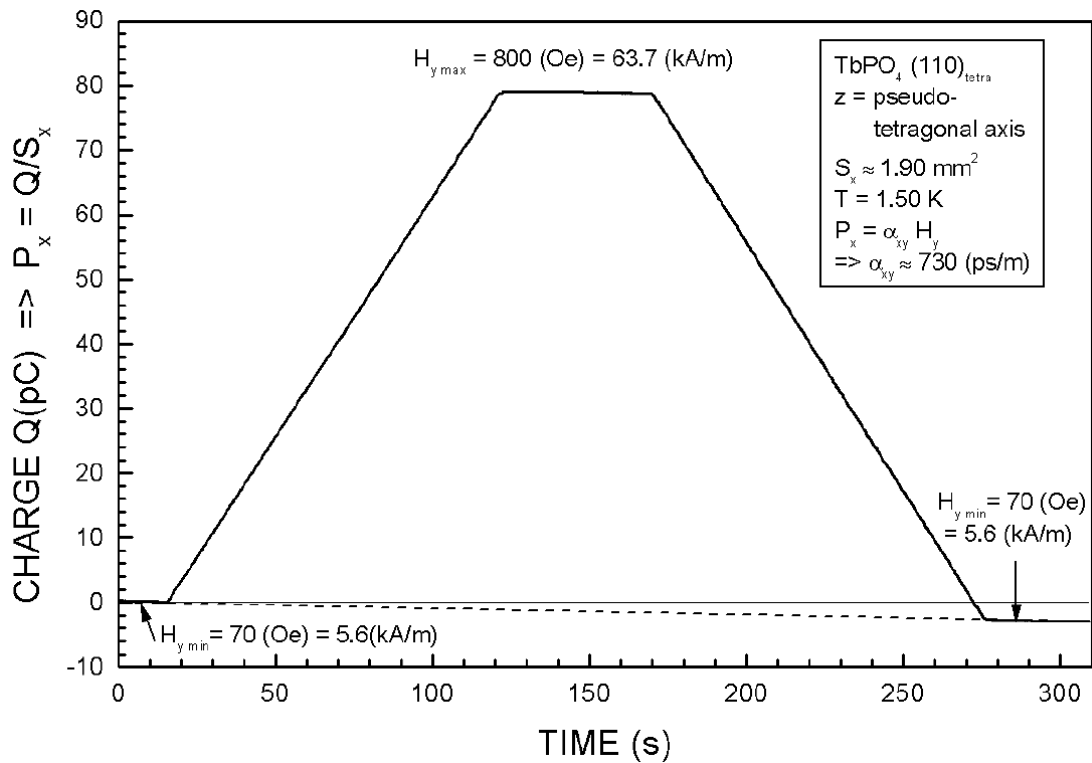


Fig. 6. $\text{TbPO}_4 (110)_{tetra}$ single crystal after ME annealing. Charge measurement $Q(\text{time})$, at $T = 1.50 \text{ K}$, with the procedure described in the text (i) to test if we have a linear or quadratic ME effect or both, here a linear ME effect only and (ii) to compute, here only the linear ME component, after correction of the small drift. The ME linear coefficient is the largest of any other single crystals known.

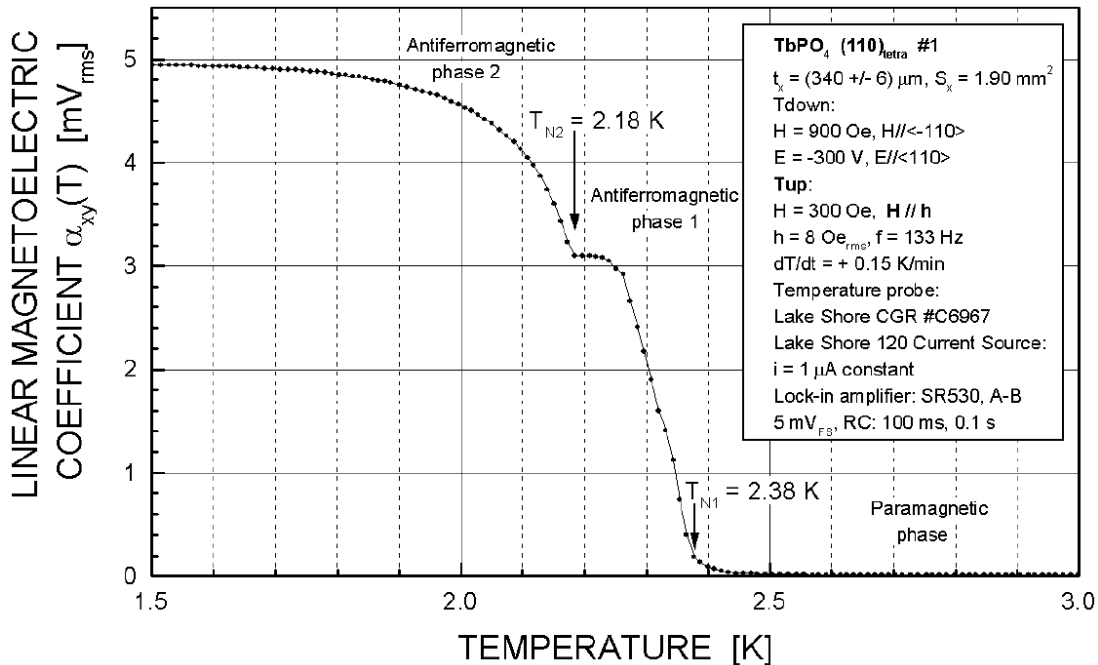


Fig. 7. $\text{TbPO}_4 (110)_{tetra}$ single crystal after ME annealing. Dynamic ME_H measurement of $\alpha_{xy}(T)$ (or $\alpha_{yx}(T)$) (a.u.), at constant magnetic fields, with a small DC magnetic field, to maintain the domains during heating, superimposed and parallel to the AC magnetic field. Both magnetic phase transitions ($T_{N2} = 2.18 \text{ K}$ and $T_{N1} = 2.38 \text{ K}$) are well observed in a narrow temperature interval of only 0.20 K .

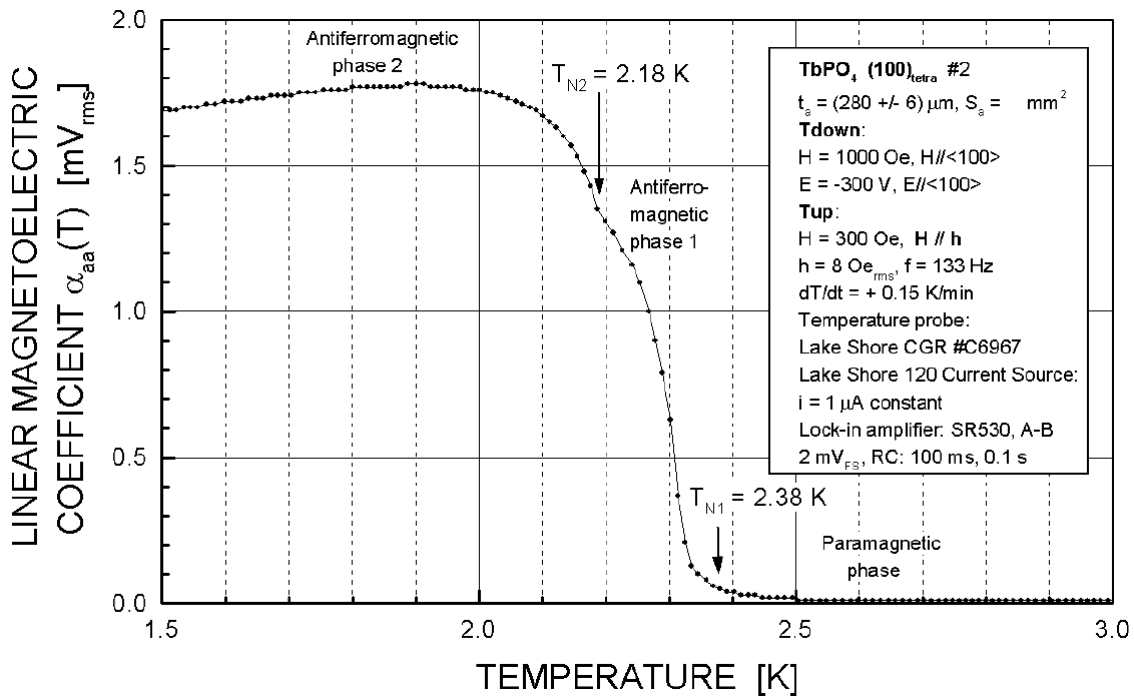


Fig. 8. TbPO₄ (100)_{tetra} single crystal after ME annealing. Dynamic ME_H measurement of $\alpha_{aa}(T)$ (a.u.) at constant magnetic fields, with a small DC magnetic field, to maintain the domains during heating, superimposed and parallel to the AC magnetic field. The magnetic phase transition $T_{N2} = 2.18 \text{ K}$ is not so well observed than with crystal #1, as in reference [11].

by dividing by 4π the value in the Gaussian units. Rado et al. in [69] found in the monoclinic magnetic phase with a tetragonal cut: $\alpha_{aa}(1.92 \text{ K}) \approx 0.011$. Thus the value they gave was in “rationalized” Gaussian units! In Figure 7 the temperature dependence of α_{xy} (or α_{yx}) is represented, measured with a dynamic ME_H method. We see very well the two phase transitions, at $T_{N2} \approx 2.18 \text{ K}$ and at $T_{N1} \approx 2.38 \text{ K}$, respectively. Note that the linear ME effect is measured in a range of temperatures of less than 1 K and that the magnetic phase between T_{N1} and T_{N2} exists only in a temperature interval of $\Delta T \approx 0.20 \text{ K}$. The ME linear coefficient of TbPO₄ is 24 times larger than $\alpha_{yx}(4.2 \text{ K})$ of LiCoPO₄ [74]. In Figure 8, α_{aa} of TbPO₄ is displayed as a function of temperature. It is consistent with the experiments described in reference [11], with a maximum near 2.0 K. The $T_{N2} = 2.18 \text{ K}$ magnetic phase transition is also much less pronounced than in the case of $\alpha_{xy}(T)$. The surface of this crystal had some defects which prevented us to measure the absolute value of α_{aa} .

The author wishes to express his thanks to Prof. Hans Schmid (University of Geneva) for suggesting this short review and for corrections and suggestions to this text, to Prof. Friedrich W. Hehl (Universities of Cologne and Missouri (Columbia)) for our recent collaboration, for corrections and suggestions to this text and to Prof. H.G. Kahle (University of Karlsruhe) for providing TbPO₄ crystals. Financial help from the organizers of the MEIPIC6 workshop, held at Santa Barbara, Jan. 25–28, 2009, is also gratefully acknowledged.

References

1. B.B. van Aken, J.-P. Rivera, H. Schmid, M. Fiebig, *Nature* **449**, 702 (2007); B.B. van Aken, J.-P. Rivera, H. Schmid, M. Fiebig, *Phys. Rev. Lett.* **101**, 157202 (2008)
2. E. Ascher, H. Rieder, H. Schmid, H. Stössel, *J. Appl. Phys.* **37**, 1404 (1966)
3. E. Ascher, *Phil. Mag.* **17**, 149 (1968)
4. E. Ascher, A.G.M. Janner, *Phys. Lett. A* **29**, 295 (1969)
5. E. Ascher, *Phys. Lett. A*, **46**, 125 (1973)
6. E. Ascher, in *Proceedings of the Symposium on Magnetoelectric Interaction Phenomena in Crystals* (MEIPIC1) (Seattle, WA USA, 1973); E. Ascher, *Int. J. Magn.* **5**, 287 (1974)
7. D.N. Astrov, *Zh. Exp. Teor. Fiz.* **38**, 984 (1960) [*Soviet Phys. JETP* **11**, 708 (1960)]
8. D.N. Astrov, *Zh. Exp. Teor. Fiz.* **40**, 1035 (1961) [*Soviet Phys. JETP* **13**, 729 (1961)]
9. A. Authier, Section 1.1.4.6.3, The method of direct inspection, *International Tables for Crystallography*, edited by A. Authier (Kluwer Academic, Dordrecht, 2003), Vol. D
10. N. Bloembergen, S.L. Hou, *Bull. Amer. Phys. Soc.* **9**, 13 (1964)
11. S. Bluck, H.G. Kahle, *J. Phys. C: Solid State Phys.* **21**, 5193 (1988)
12. J. van den Boomgaard, A.M.J.G. van Run, J. van Sachtelen, *Ferroelectrics* **10**, 295 (1976)
13. A.S. Borovik-Romanov, *Soviet Phys. JETP* **9**, 1390 (1959), translation of *J. Expt. Theo. Phys. (U.S.S.R.)* **36**, 1954 (1959)
14. A.S. Borovik-Romanov, H. Grimmer, Section 1.5.8, Magnetoelectric effect, *International Tables for Crystallography*, edited by A. Authier (Kluwer Academic, Dordrecht, 2003), Vol. D

15. P. Borisov, A. Hochstrat, V.V. Shvartsman, W. Kleemann, *Rev. Sci. Instr.* **78**, 106105 (2007)
16. W.F. Brown, R.M. Hornreich, S. Strikman, *Phys. Rev.* **168**, 574 (1968)
17. W.F. Brown, *IEEE Trans. Magnetics* **MAG-20**, 112 (1984)
18. M. Clin, J.-P. Rivera, H. Schmid, *Ferroelectrics* **79**, 173 (1988)
19. M. Clin, J.-P. Rivera, H. Schmid, *Ferroelectrics* **108**, 207 (1990)
20. M. Clin, J.-P. Rivera, H. Schmid, *Ferroelectrics* **108**, 213 (1990)
21. P. Curie, *J. Physique*, 3^{ième} série III, 393 (1894) (Reprinted in *Œuvres de Pierre Curie* (Gauthier-Villars, Paris, 1908), pp. 118–141)
22. I.E. Dzyaloshinskii, *Zh. Exp. Teor. Fiz.* **37**, 881 (1959) [*Soviet Phys. JETP* **10**, 628 (1960)]
23. C. Ederer, N.A. Spaldin, *Phys. Rev. B* **76**, 214404 (2007)
24. C. Ederer, *this Conference, Magnetoelectric Interaction Phenomena in Crystals (MEIPIC6)* (University of California, Santa Barbara CA, 2009)
25. M. Fiebig, K. Kohn, S. Leute, T. Lottermoser, V.V. Pavlov, R.V. Pisarev, *Phys. Rev. Lett.* **84**, 5620 (2000)
26. M. Fiebig, *J. Phys. D: Appl. Phys.* **38**, R123 (2005)
27. J. Fischer, *Größen und Einheiten der Elektrizitätslehre* (Springer, Berlin, 1961)
28. V.J. Folen, G.T. Rado, E.W. Stalder, *Phys. Rev. Lett.* **6**, 607 (1961)
29. F.G. Fumi, *Acta Cryst.* **5**, 44 (1952); F.G. Fumi, *Acta Cryst.* **5**, 691 (1952)
30. A.A. Gorbatsevich, Y.V. Kopaev, *Ferroelectrics* **161**, 321 (1994)
31. H. Grimmer, *Acta Cryst. A* **47**, 226 (1991)
32. H. Grimmer, *Acta Cryst. A* **48**, 266 (1992)
33. H. Grimmer, *Ferroelectrics* **161**, 181 (1994)
34. E.A. Guggenheim, *Thermodynamics*, 8th edn. (North-Holland, Amsterdam, 1985)
35. G. Harshé, J.P. Dougherty, R.E. Newnham, *Int. J. Appl. Electromagnetics in Materials* **4**, 145 (1993); G. Harshé, J.P. Dougherty, R.E. Newnham, *Int. J. Appl. Electromagnetics in Materials* **4**, 161 (1993)
36. G. Harshé, personal communication (1994)
37. F.W. Hehl, Y.N. Obukhov, *Foundations of Classical Electrodynamics* (Birkhäuser, Boston, 2003)
38. F.W. Hehl, Y.N. Obukhov, *Gen. Relativ. Gravit.* **37**, 733 (2005)
39. F.W. Hehl, Y.N. Obukhov, J.-P. Rivera, H. Schmid, *Phys. Rev. A* **77**, 022106 (2008)
40. F.W. Hehl, Y.N. Obukhov, J.-P. Rivera, H. Schmid, in *Proceedings of MEIPIC6* (2009), to appear in *Eur. Phys. J. B*
41. F.W. Hehl, private communication (2009)
42. S.L. Hou, N. Blombergen, *Phys. Rev.* **138**, A1218 (1965)
43. *International Tables for Crystallography, Space-group symmetry*, 5th edn., reprinted edn. T. Hahn (Kluwer Academic, Dordrecht, 2005), Vol. A
44. J.D. Jackson, *Classical Electrodynamics*, 3rd edn. (John Wiley, New York, 1999)
45. H.G. Kahle, S. Bluck, A. Kasten, *J. Mag. Mag. Materials* **54**, 1327 (1986)
46. H.G. Kahle, *Ferroelectrics* **161**, 295 (1994)
47. N.F. Kharchenko, *Ferroelectrics* **162**, 173 (1994)
48. N.F. Kharchenko, Y.N. Kharchenko, R. Szymczak, M. Baran, H. Schmid, *Low Temp. Phys.* **27**, 895 (2001) (Translation of *Fizika Nizkikh Temperatur* (Kiev))
49. N.F. Kharchenko, V.A. Desnenko, Y.N. Kharchenko, R. Szymczak, M. Baran, *Low Temp. Phys.* **28**, 646 (2002) (Translation of *Fizika Nizkikh Temperatur* (Kiev))
50. Y. Kharchenko, N. Kharchenko, M. Baran, R. Szymczak, *Magnetoelectric Interaction Phenomena in Crystals (MEIPIC-5)*, edited by M. Fiebig et al. (Kluwer-Academic, Dordrecht, 2004), p. 227
51. E. Kita, *Ferroelectrics* **162**, 397 (1994)
52. I. Kornev, M. Bichurin, J.-P. Rivera, S. Gentil, H. Schmid, *Phys. Rev. B* **62**, 12247 (2000)
53. L.D. Landau, E.M. Lifshitz, *Electrodynamics of Continuous Media*, of Course of Theoretical Physics, 2nd edn., transl. from the Russian (Pergamon, Oxford, 1984), Vol. 8
54. Landolt-Börnstein, *Numerical Data and Functional Relationships in Science and Technology*, New Series, Group III, edited by K.-H. Hellwege (Springer, Berlin, 1982), Vol. 12, Part c
55. D.B. Litvin, *Acta Cryst. A* **64**, 316 (2008)
56. D.B. Litvin, *Acta Cryst. A* **64**, 419 (2008)
57. Quoting footnote 3 in D.B. Litvin [56], on p. 422: "This electronic book is available from the IUCr electronic archives (Reference: PZ5052). This electronic book may also be downloaded from <http://www.bk.psu.edu/faculty/Litvin/download.html> and is also available on CD on request from the author (D.B. Litvin), email: u3c@psu.edu
58. Maple8 or Maple12, Maplesoft, Waterloo, Ontario, Canada, <http://www.maplesoft.com>
59. J.F. Nye, *Physical Properties of Crystals, Their Representation by Tensors and Matrices* (Oxford University Press, 1990)
60. T.H. O'Dell, *Phil. Mag.* **16**, 487 (1967)
61. T.H. O'Dell, *The Electrodynamics of Magneto-Electric Media* (North-Holland, Amsterdam, 1970)
62. W.K.H. Panofsky, M. Phillips, *Classical Electricity and Magnetism* (Addison-Wesley, Reading, MA, USA, 1964)
63. E.J. Post, *Formal Structure of Electromagnetics-General Covariance and Electromagnetics* (North-Holland, Amsterdam, 1962) and (Dover, Mineola, NY, 1997)
64. R.E. Raab, E.B. Graham, *Ferroelectrics* **204**, 157 (1997)
65. G.T. Rado, V.J. Folen, *Phys. Rev. Lett.* **7**, 310 (1961)
66. G.T. Rado, V.J. Folen, *J. Phys. Soc. Jpn*, Suppl. B-I **17**, 244 (1962)
67. G.T. Rado, *Phys. Rev.* **128**, 2546 (1962)
68. G.T. Rado, *Phys. Rev. B* **15**, 290 (1977)
69. G.T. Rado, J.M. Ferrari, W.G. Maisch, *Phys. Rev. B* **29**, 4041 (1984)
70. J.-P. Rivera, H. Schmid, *Ferroelectrics* **36**, 447 (1981)
71. J.-P. Rivera, H. Schmid, *Ferroelectrics* **55**, 295 (1984)
72. J.-P. Rivera, H. Schmid, *J. Appl. Phys.* **70**, 6410 (1991)
73. J.-P. Rivera, H. Schmid, *Ferroelectrics* **161**, 91 (1994)
74. J.-P. Rivera, *Ferroelectrics* **161**, 147 (1994)
75. J.-P. Rivera, *Ferroelectrics* **161**, 165 (1994)
76. R.P. Santoro, D.J. Segal, R.E. Newnham, *J. Phys. Chem. Solids* **27**, 1192 (1966)
77. D.G. Sannikov, *Zh. Eksp. Teor. Fiz.* **111**, 536 (1997) [*JETP* **84**, 293 (1997)]
78. D.G. Sannikov, *Ferroelectrics* **219**, 177 (1998)

79. D.G. Sannikov, Pis'ma Zh. Eksp. Teor. Fiz. **73**, 447 (2001), [JETP Lett. **73**, 401 (2001)]
80. D.G. Sannikov, Zh. Eksp. Teor. Fiz. **120**, 661 (2001), [JETP **93**, 579 (2001)]
81. H. Schmid, in Russian: Rost Kristallov **7**, 32 (1967), in English: *Crystal Growth*, editet by N.N. Sheftal, (Consultants Bureau, New York, 1969), Vol. 7, p. 25
82. H. Schmid, Phys. Stat. Sol. **37**, 209 (1970)
83. H. Schmid, *Proceedings of the Symposium on Magnetoelectric Interaction Phenomena in Crystals (MEIPIC1)* (Seattle, WA, 1973); H. Schmid, Int. J. Magn. **4**, 239 (1973)
84. H. Schmid, Ferroelectrics **162**, 317 (1994)
85. H. Schmid, Ferroelectrics **221**, 9 (1999)
86. H. Schmid, in *Introduction to Complex Mediums for Optics and Electromagnetics*, edited by W.S. Weiglhofer, A. Lakhtakia (SPIE Press, Bellingham, WA, 2004), p. 167
87. H. Schmid, J. Phys.: Condens. Matter **20**, 434201 (2008)
88. W. Schnelle, E. Gmelin, O. Crottaz, H. Schmid, J. Therm. Anal. Cal. **56**, 365 (1999)
89. S. Shtrikman, D. Treves, Phys. Rev. **130**, 986 (1963)
90. V.V. Shvartsman, S. Bedanta, P. Borisov, W. Kleemann, A. Tkach, P.M. Vilarinho, Phys. Rev. Lett. **101**, 165704 (2008)
91. A. Sommerfeld, *Lectures on Theoretical Physics, Electrodynamics* (Academic Press, New York, 1952), Vol. III
92. A. Sommerfeld, *Lectures on Theoretical Physics, Thermodynamics and Statistical Mechanics* (Academic Press, New York, 1956), Vol. V
93. N.A. Spaldin, M. Fiebig, M. Mostovoy, J. Phys.: Condens. Matter **20**, 434203 (2008)
94. *IEEE Standard on Piezoelectricity* (ANSI/IEEE Std 176-1987) (The Institute of Electrical and Electronics Engineers, New York, 1988); also reproduced in *Piezoelectricity*, edited by C.Z. Rosen, B.V. Hiremath, R.E. Newnham (Key Papers in Physics Series, American Institute of Physics, New York, 1992), pp. 227-280
95. J. van Suchtelen, Philips Res. Rep. **27**, 28 (1972)
96. M. Tinkham, *Group Theory and Quantum Mechanics* (McGraw-Hill, New York, 1964)
97. *Magnétisme*, edited by E. du Trémolet de Lacheisserie (Presses Universitaires de Grenoble, Grenoble, France, 1999)
98. IUPAP "Red book" "Symbols, Units, Nomenclature, Atomic Masses & Fundamental Constants", (IUPAP Commission C2 SUNAMCO, 1987), http://www.sp.se/metrology/IUPAP_SUNAMCO/IUPAP_SUNAMCO_Commission.htm, see also <http://physics.nist.gov/cuu/Constants/index.html> the Web site of the National Institute on Standards and Technology
99. D. Vaknin, J.L. Zaresky, L.L. Miller, J.-P. Rivera, H. Schmid, Phys. Rev. B **65**, 224414 (2002)
100. W. Voigt, *Lehrbuch der Kristallphysik, mit Ausschluss der Kristalloptik* (Johnson Reprint Corp., New York, 1966; Teubner, Leipzig, reprinted 1946, first edition, 1910)
101. H. Wiegelmann, *Magnetoelectric Effects in Strong Magnetic Fields*, Ph.D. Thesis, University of Konstanz (Hartung-Gorre Verlag, Konstanz, 1994)
102. M.W. Zemansky, *Heat and Thermodynamics* (McGraw-Hill, New York, 1957)
103. W. Zinn, Section 6.0.3.3, Magnetic fields and units, in *Landolt- Börnstein, Numerical Data and Functional Relationships in Science and Technology*, edited by K.-H. Hellwege, New Series *Magnetic and Other Properties of Oxides and Related Compounds* (Springer, Berlin, 1982), Group III, Part c, Vol. 12, p. 56